Bulletin of the Seismological Society of America, Vol. 85, No. 6, pp. 1665–1678, December 1995

Why the L_g Phase Does Not Traverse Oceanic Crust

by Tian-Run Zhang and Thorne Lay

Abstract It has long been recognized that L_g waves are not observed on paths traversing oceanic crust, but this has not yet been fully explained. Using normal-mode analysis and finite-difference simulations, we demonstrate that (1) the overall thickness of the crustal wave guide affects the number of normal modes in a given frequency range; in general, thinner crust accommodates fewer modes; (2) 6-km-thick oceanic crust does not allow L_g to develop as a significant phase in the frequency band 0.3 to 2 Hz because of the limited number of modes that exist; (3) in continental crust thicker than 15 km, there are usually sufficient modes that L_g is stable; (4) the shallow sediment layer plays important roles in crustal-guided wave propagation, trapping energy near the surface, separating L_g and R_g waves; (5) a 100-km-long segment of oceanic structure on a mixed ocean/continent path can block *P–SV* type L_g propagation. The primary reason why L_g does not travel through oceanic crust thus lies in the structure of the crustal wave guide, with the decisive factor being the crustal thickness. The detailed shape of ocean-to-continent crustal transitions can influence L_g blockage, but the general inefficiency of L_g propagation in the oceanic structure is the dominant effect.

Introduction

Early observations detected L_g extinction when the propagation path included an oceanic portion with length greater than 100 to 200 km (Press and Ewing, 1952). However, the reason why L_g only propagates in continental crust still remains unclear after four decades, and the basis for characterizing crustal structure using L_g propagation efficiency has been questioned (Regan and Harkrider, 1989a).

Ewing *et al.* (1957) hypothesized that the disappearance of L_g in oceanic regions might be due to the effect of propagation across a continent-ocean margin. Kennett (1986) has illustrated this hypothesis with ray diagrams. There is no doubt that initially trapped L_g energy will radiate out of the crust when passing through a tapered wave guide, as the varying geometry allows some postcritical raypaths to become precritical (e.g., Kock, 1965; Bostock and Kennett, 1990). If this is the main reason, the structure of the continental margins would play a more important role than the structure of the oceanic crust itself in disrupting L_g propagation. However, there have been observations along purely oceanic paths in the Atlantic and Pacific (for earthquakes at trenches and receivers on small islands) that show no short-period L_g arrivals (Knopoff *et al.*, 1979). Knopoff *et al.* (1979) found that clustering of higher-mode group velocity minima (the generally recognized cause of the L_g phase (e.g., Knopoff *et al.*, 1973)) is absent in simple oceanic crustal structures. This suggests that the reason for L_g not being observed on paths with mixed continental and oceanic crust may lie in the structure of oceanic crust, rather than in the details of the continental margin. We will explore this issue using synthetic seismograms for both one-dimensional crustal models and two-dimensional continent-ocean transitions in this study.

The importance of understanding crustal wave-guide controls on L_g has prompted several modeling studies of blockage, but the observations have been hard to simulate (Maupin, 1989; Regan and Harkrider, 1989a, 1989b; Campillo *et al.*, 1993; Chazalon *et al.*, 1993; Gibson and Campillo, 1994). These authors argue that unmodeled small-scale heterogeneity is needed to account for the blockage rather than large-scale wave-guide structure. Recently, Cao and Muirhead (1993) used a two-dimensional *P–SV* finite-difference method to explore L_g blockage. Because the reduction of L_g obtained in models that involve a segment of thinned crust is not as strong as required by observations, they introduced a water layer overlying the thinned crust that further reduces the energy they identify as L_g. We perform finite-difference calculations similar to those of Cao and Muirhead (1993) and draw somewhat different conclusions in this study by taking care to separate the effects of wave-guide structure on L_g and R_g.

In this article, we consider the basic nature of L_g in oceanic and continental wave guides along with further investigation of L_g blockage for the *P–SV* component. We use normal-mode analysis and a two-dimensional fourth-order elastic wave finite-difference method (Xie and Yao, 1988) to construct dispersion curves and synthetic velocity seis-

mograms for L_g in one- and two-dimensional crustal models. Our basic objective is to improve our understanding of the relative efficiency of L_g excitation and propagation in oceanic and continental structures.

Crustal Thickness and the Number of Normal Modes

To first order, we can view the crust as a low-velocity layer over a higher-velocity half-space. In such a simple system, the L_g phase can be visualized either as trapped postcritical reflections (e.g., Campillo, 1990) or, equivalently, as Rayleigh and Love wave overtones (e.g., Kovach and Anderson, 1964; Knopoff *et al.*, 1973). In the latter interpretation, it is necessary to consider a substantial number of overtones to produce the complexity and interference characterizing the L_g phase. It is well known that as wave-guide thickness and/or frequency decrease, the number of surface-wave overtones reduces (e.g., Marcuse, 1991, p. 12). Aki and Richards (1980, p. 264) give the traditional formula for calculating the cutoff frequency of the nth higher-mode ω_{cn} for the case of Love waves in a simple layer over a half-space model:

$$\omega_{cn} = \frac{n\pi\beta_1}{H\left(1 - \frac{\beta_1^2}{\beta_2^2}\right)^{1/2}}, \tag{1}$$

where H is the thickness of the crustal layer (wave guide), β_1 is the shear-wave velocity in the wave guide, β_2 is the shear-wave velocity in the half-space, n is the order number of that higher mode. This expression is commonly used for fixed H and n. Alternatively, if we specify a maximum frequency and the layer thickness, we can express the maximum number of viable overtones in the system, n_c, as

$$n_c = \frac{\omega H}{\pi\beta_1}\left(1 - \frac{\beta_1^2}{\beta_2^2}\right)^{1/2}, \tag{2}$$

with truncation to an integer value being assumed. Equation (2) shows that the maximum number of normal modes up to a particular frequency is determined by the wave-guide thickness and the wave velocities. The corresponding solution for the number of Rayleigh wave overtones up to a certain frequency is similar but more complicated. Fewer normal modes exist as thinner wave guides are considered. The existence of the Rayleigh wave fundamental mode does not depend on the wave-guide thickness, and even when the thickness is so small that no higher modes can propagate in the wave guide, the fundamental mode will still exist (e.g., Brekhovskikh, 1980, p. 64).

To further explore the dependence of number of modes on crustal thickness, we calculated the Rayleigh wave dispersion curves for a simple one-layer crustal model like that in Figure 1a. We assign the crustal layer the density, S-wave velocity and P-wave velocity values corresponding to "basalt," and the half-space the parameters corresponding to "mantle," given in Table 1. These parameters follow those used by Cao and Muirhead (1993). Group velocity dispersion curves were calculated in the frequency range of 0.0 to 2.0 Hz for varying crustal thickness, using the codes developed by Herrmann and Wang (1985). For a 32-km-thick crust (Fig. 2a), the group velocity minima (or Airy phases) concentrate within a narrow group velocity range between 3 and 3.5 km/sec. The concentrated L_g phase develops by constructive interference of these higher-mode Airy phases. The fundamental-mode Airy-phase group velocity is slightly lower than that of any of the overtones, so there will be some separation of the L_g phase and the R_g phase, but not very much for this model.

As the thickness decreases, the cutoff frequencies for the dispersion curves shift to higher frequencies, reducing the number of overtones. For the 0- to 2-Hz band, there are 24 modes for a 32-km-thick crust, 19 modes for a 25-km-thick crust, 12 modes for a 15-km-thick crust, and only 5 modes for the 6-km-thick (oceanic) crust (Fig. 2). With the velocities of crust and mantle being held fixed, the Airy-phase group velocities do not vary significantly. The number-of-modes versus layer thickness behavior of Rayleigh waves for constant velocity models clearly exhibits a quasi-linear relationship. As expected from equation (2), Love waves display a similar behavior.

This simple calculation holds no surprises, but it does

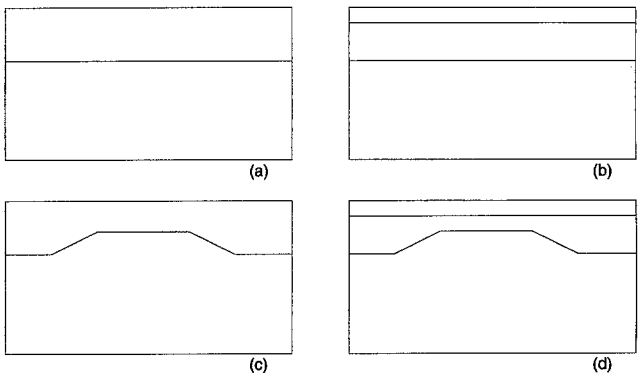

Figure 1. Four categories of crustal model used in this study including (a) a layer over half-space model; (b) a two-layer crust model, with a sediment layer added on top of model (a); (c) a model with a segment of thin crust; (d) a model with a segment of thin crust and a sediment layer.

Table 1
Model Parameters Used in Finite-Difference Simulation

	Density (gm/cm³)	S-wave velocity (km/sec)	P-wave velocity (km/sec)
Sediment	2.2	2.60	4.50
Basalt	2.8	3.58	6.20
Mantle	3.4	4.73	8.20

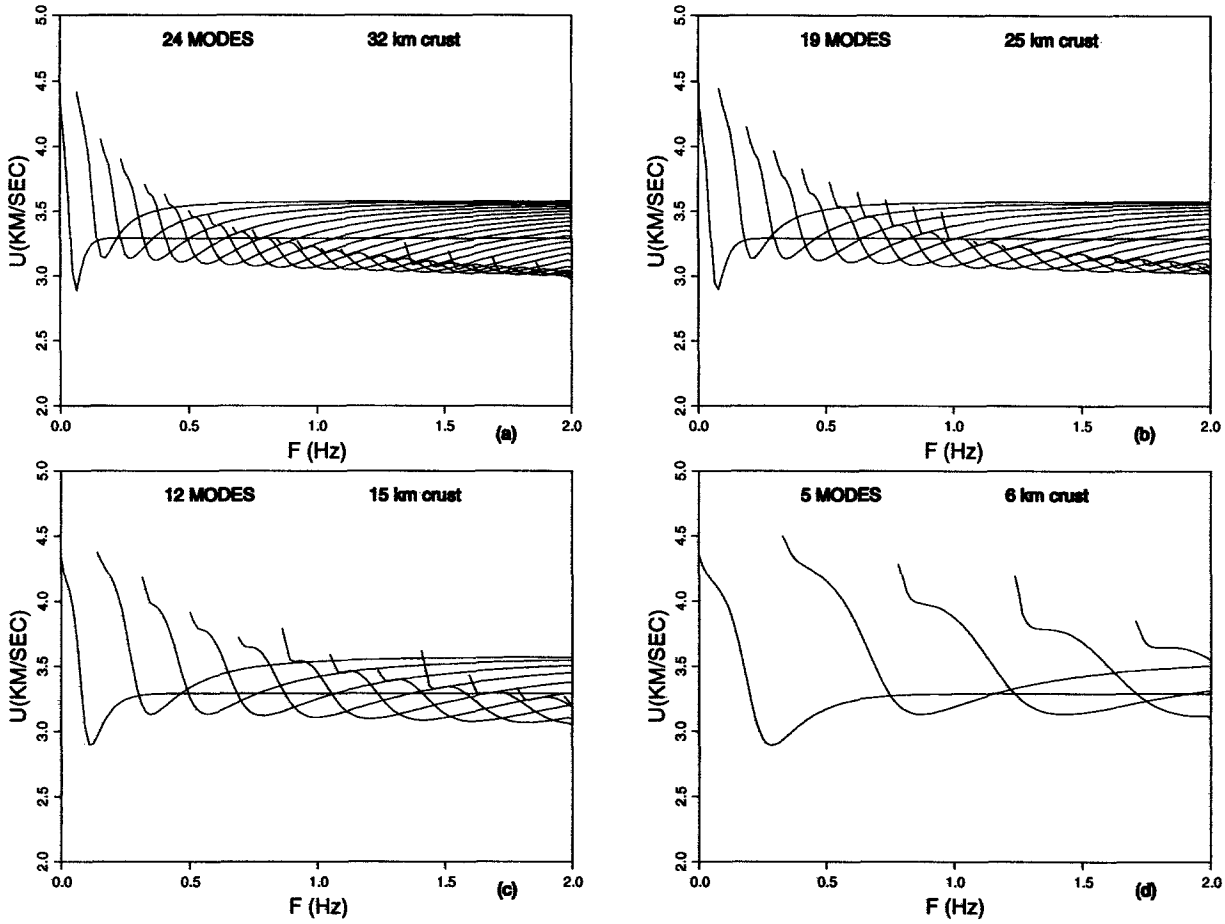

Figure 2. Dispersion curves for Rayleigh waves in layer over half-space models with crustal thickness of (a) 32 km, (b) 25 km, (c) 15 km, and (d) 6 km. U stands for group velocity. The number of normal modes in the 0 to 2 Hz range decreases for thinner crust.

focus attention on the issue that the development of the L_g phase will depend on the number of interfering modes, which is strongly influenced by crustal thickness. To some extent, this issue has not been carefully considered in many of the investigations of wave-guide effects on L_g.

L_g Synthetics for 1D Models

In this section, we explore further the effects of gross one-dimensional homogeneous wave-guide structure on L_g wave propagation. We do not introduce intrinsic attenuation or small-scale scattering in our calculations, although these are undoubtedly important effects for L_g in the Earth. Following Xie and Lay (1994), a Gaussian derivative source-time history, $(t - t_s)\exp[-(t - t_s)^2/\tau^2]$, is used for all of the finite-difference calculations, where t_s is a reference time and τ is the characteristic width of the source pulse. We use $\tau = 0.5$ sec in all the calculations. The main energy of this source-time history is between 0.1 and 1.0 Hz, which is the frequency band relevant to the majority of observational studies of L_g propagation. Press and Ewing (1952) originally defined L_g within the 0.17- to 2.0-Hz band, and many of the applications of L_g for magnitude measures (e.g., Nuttli, 1986) use 1-Hz L_g amplitudes. Many early theoretical studies of L_g (e.g., Knopoff *et al.*, 1973; Panza and Calcagnile, 1975) compute synthetics for the frequency range less than 1 Hz, similar to the calculations given in the following section.

Layer over Half-Space Models

In the previous section, we showed that wave-guide thickness influences the number of modes in a given frequency band. While it makes sense that there will be a corresponding effect on the time-domain amplitude of L_g, it is important to assess how strong this effect is. We perform finite-difference calculations for the same crustal models used for the earlier dispersion calculations, in order to construct complete seismograms for a realistic source. Normal-mode calculations could have been used to produce the synthetic seismograms, but the finite-difference approach has the advantage of readily including all of the body-wave phases that provide references for the L_g amplitudes. For all models explored in this article, the source is located at the

left end of the model at a depth of 5 km. The source is a 45° dip-slip dislocation for all finite-difference calculations. Synthetic seismograms are calculated at 18 locations with spacing of 20 km on the free surface, starting 100 km away from the source and ending at 440 km. In this distance range, L_g evolves from discrete crustal reverberations to a complex interference pattern.

Figure 3 shows synthetic seismograms for both radial and vertical components for a constant velocity ("basalt" parameters), single-layer, 32-km-thick crust model. The two reference lines indicate the group velocity window 3.7 to 3.1 km/sec, which is commonly used for RMS L_g calculation (e.g., Israelson, 1992; Zhang and Lay, 1994a, 1994b; Zhang *et al.,* 1994). This is called the "L_g window," although in a strict sense, it may only be valid for typical continental crust, given that overtone group velocities in oceanic structure may differ from those in the continents. The two major regional surface-wave phases, R_g and L_g, overlap within the L_g window because the group velocity of the fundamental mode Airy phase is only slightly lower than that of the higher modes (Fig. 2a). The R_g phase is dominated by lower-frequency energy and has the largest amplitudes in the L_g window, with the vertical component being stronger than the radial component. The mix of Rayleigh wave arrivals in the L_g window has amplitudes comparable to the P_g phase on the radial components.

To verify the coexistence of the two phases (L_g and R_g), we consider particle motions for the arrivals within the L_g window (Fig. 4). Figure 4a shows waveforms of the two components in the L_g window. Treating the radial amplitudes as x coordinates and vertical amplitudes as y coordinates, we convert the (x, y) pairs to (r, θ) polar coordinates and show the variation of θ with time in Figure 4b. If the particle motions are retrograde ellipses, the phase angle θ must increase monotonically from 0 to 2π, then wrap around. The early part of the seismogram segment shown in Figure 4a

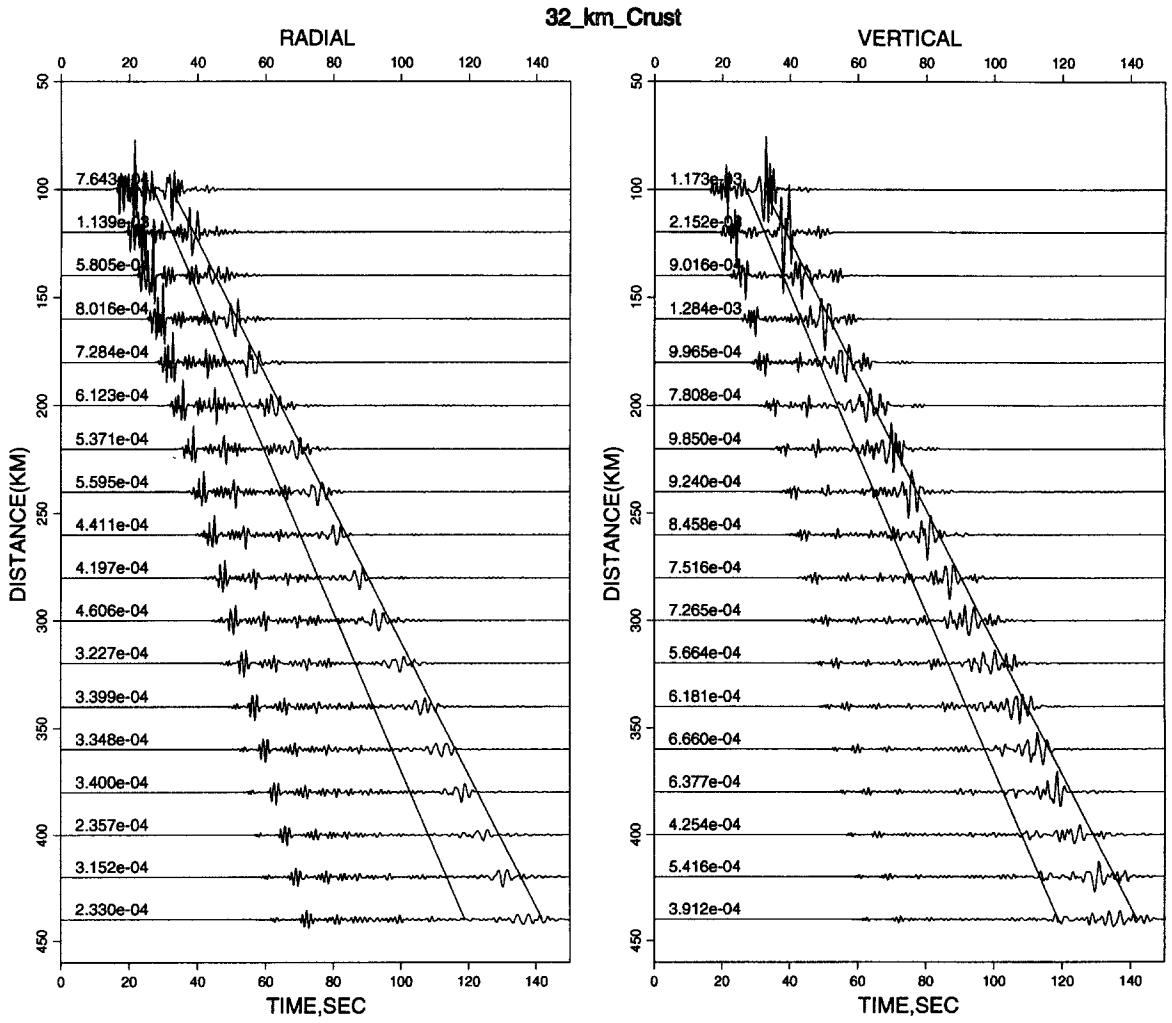

Figure 3. Synthetic seismograms for a layer over half-space model with 32-km-thick crust. Both radial and vertical components are shown. Two lines mark the group velocity window 3.7 to 3.1 km/sec used for calculation of RMS L_g amplitudes (called the L_g window). The RMS amplitude values in the L_g window are shown for each waveform.

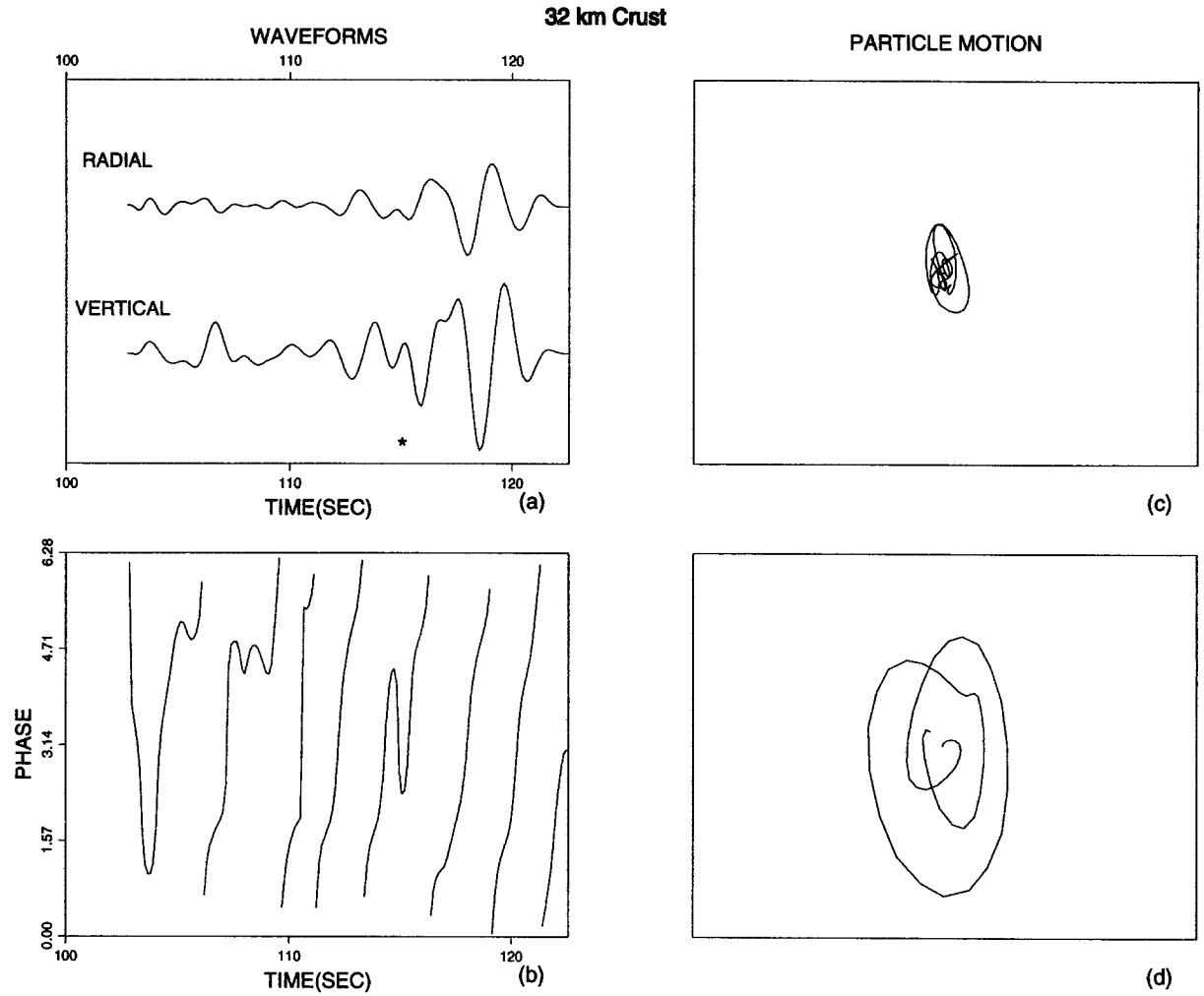

Figure 4. Particle motions in the L_g window for the waveform at 380-km distance in Figure 3: (a) shows the radial and vertical components in the L_g window. The asterisk marks a transition in characteristic particle motion, and (b) is the polarization angle as a function of time (see text). Both (c) and (d) are the particle motions of the early part of the L_g window before the asterisk and the late part of the L_g window, respectively. R_g dominates the late part, while higher modes dominate the early part.

exhibits complex phase, while the later part is predominantly retrograde elliptical, with smoothly increasing phase (Fig. 4b). The asterisk on Figure 4a marks the approximate transition between the two domains. The particle motions for the two separate waveform intervals are shown in Figures 4c and 4d. The later part is predominantly the R_g arrival, but there is some higher-mode energy present, which makes the ellipses irregular. The early part shows complex, interfering motions that imply the presence of the multiple arrivals constituting L_g, but there is some elliptical motion indicating contribution from the fundamental mode within the L_g window. We calculate RMS amplitudes for the L_g window, recognizing that in some models, there is contamination by R_g.

We constructed synthetic profiles for models with crustal thicknesses of 25 and 15 km, finding that although the reduction of number of Rayleigh wave overtones is considerable (Fig. 2), the RMS amplitude values within L_g window are not much different than for the 32-km-thick model. The reasons are (1) R_g dominates in this window, and (2) the most important contributions to the L_g phase come from the first few modes (Knopoff *et al.*, 1973). There may be a tendency for the lower modes to enhance in strength when fewer modes fit into the system, but the overall overtone energy must begin to drop off when the number of modes becomes very small. This appears to occur as the crustal thickness becomes as small as for oceanic structure. The synthetics for a 6-km-thick crustal model (model I in Table 2) shown in Figure 5 illustrate this effect. There is almost no energy in the L_g window. Only five modes and three overtone Airy phases exist in the 0- to 2-Hz frequency range (Fig. 2d), and only one overtone has an Airy phase in the band 0 to 1 Hz. The arrivals just after the L_g window are R_g, which does not stay in the L_g window in the 6-km-thick crust case. The short-period fundamental mode energy has be-

Table 2
Six Crustal Models Used in This Model*

	Layer 1 (H/V_p)	Layer 2 (H/V_p)	Layer 3 (H/V_p)	Layer 4 (H/V_p)	Layer 5 (H/V_p)	Layer 6 (H/V_p)
I	6.0/6.2	∞/8.2				
II	2.0/4.5	4.0/6.2	∞/8.2			
III	1.0/2.10	5.0/6.41	∞/8.1			
IV	0.34/2.10	1.21/5.15	4.57/6.82	∞/8.15		
V	0.5/2.08	0.95/4.46	1.15/6.0	1.70/6.74	2.90/7.47	∞/8.28
VI	10.0/6.06	20.0/6.35	20.0/7.05	∞/8.17		

*H is the layer thickness in kilometers, V_p is the P-wave velocity in km/sec. Model I stands for a single-layer oceanic crust; II is the oceanic crust model with a 2-km-thick low-velocity layer on the top; III is the worldwide ocean crust model from Meissner (1986); IV and V are two Pacific crust models from Shor *et al.* (1970) and Hussong (1972); VI is the worldwide continent model from Meissner (1986).

come stronger relative to the body waves compared to the thicker crustal models due to the shift of the Airy-phase frequency (Fig. 2). However, with a group velocity of about 2.8 km/sec, most of this energy is now outside the L_g window. This calculation demonstrates that a thin uniform wave guide, approximating the oceanic crust, is very inefficient for the transmission of 0- to 1-Hz L_g waves, relative to the body wave and fundamental mode energy. We obtain this result without introducing a continent-ocean transition.

The RMS L_g amplitudes along profiles from 200 to 440 km for several different models are summarized in Figure 6. The solid circles and squares indicate the results for the 32- and 6-km-thick crustal models, respectively. The L_g signal is very weak in 6-km-thick crust, especially when the distance is greater than 300 km. The beating of the fundamental mode and overtones in the thicker crustal models causes the fluctuations with distance.

Crustal Models with a Sediment Layer

The presence of R_g in the L_g window, as in the synthetics in the previous section, is rarely observed. When present at all, R_g is typically significantly later than L_g, with a characteristic continental path group velocity of 3.05 ± 0.07 km/

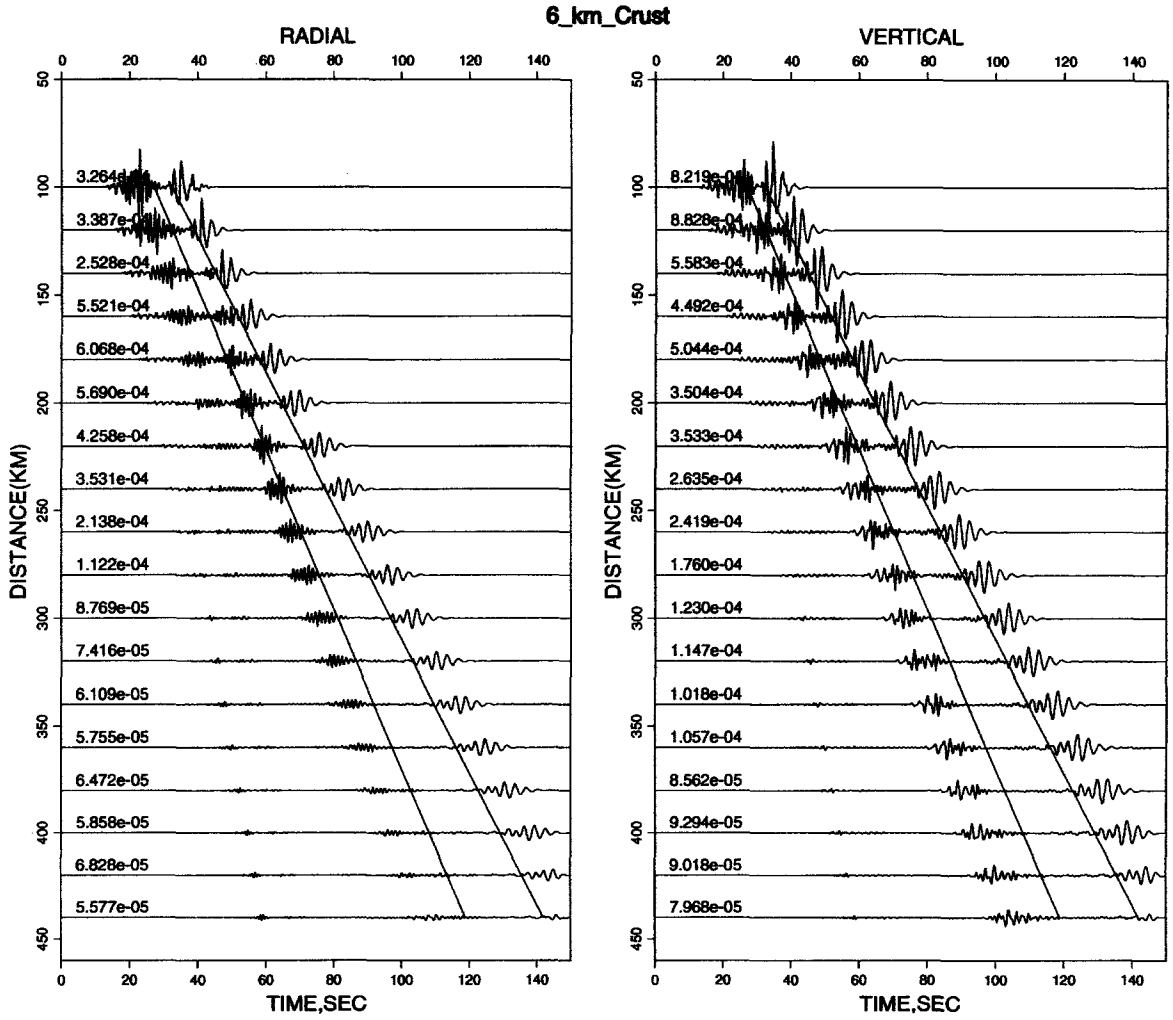

Figure 5. Synthetic seismograms for a layer over half-space model with 6-km crustal thickness. The arrivals within the L_g window are weak. The R_g waves are delayed, and most of their energy is outside the L_g window.

sec (Press and Ewing, 1952). This low group velocity is largely due to layering of the crust, in particular the presence of low-velocity surface layers. To include this in the synthetics, we add a 2-km-thick low-velocity layer at the top of each crustal model, as illustrated in Figure 1b and model II in Table 2. The velocities and density of the "sediment" layer are listed in Table 1.

The low-velocity surface layer has two effects on the Rayleigh wave modes. First, it lowers the group velocities of the Airy phases of all the modes. Second, it tends to trap shorter-period fundamental-mode energy within the shallow crust, slowing it down considerably. The dispersion curves of the fundamental mode have two minima for these three-layer models (Fig. 7). The low-frequency Airy phase is basically the same as for the single-layer crust, with a slight reduction in group velocity, because the average crustal velocities are reduced (see Fig. 2 for comparison). The second Airy phase involves the energy trapped in the surface layer and has quite low velocity over a range of periods from 2 to 1 sec. The short-period R_g amplitudes are now quite strong, as illustrated by the synthetic seismograms for a 32-km-thick crustal model shown in Figure 8. From the dispersion curves for different crustal thicknesses (Fig. 7), we find that the first higher mode has a similar double minima at higher frequency, but other modes do not change much compared with models without the sediment layer in the 0 to 2 Hz range. As a result of the low-velocity layer, L_g and R_g are separated in the time domain. This separation eliminates the overlap of L_g and R_g in the L_g window. Analysis of the particle motions now shows complex interfering motion throughout the L_g window (Figs. 9b and 9c), implying the clustering of higher modes. The R_g arrival, concentrated in the following time interval, shows stable retrograde elliptical motion (Figs. 9b and 9d). Aside from this delay of R_g, the behavior of the RMS L_g amplitudes as a function of overall wave-guide thickness is very much the same as described for the single-layer crust. Using synthetic profiles computed for each of the crustal thicknesses in Figure 7, RMS L_g amplitudes were computed at each distance and are shown by open symbols in Figure 6. While RMS amplitudes in the L_g window are systematically reduced relative to the single-layer crustal models, the result of R_g being delayed out of the window, the L_g amplitudes are still much higher (by a factor of 4 to 5) for the thicker crusts than for the oceanic-type crust. Figure 7 suggests that the reason for this is still the reduction of the number of overtones with which to build up the L_g phase. The beating patterns with distance are reduced in Figure 6 because there is much less interference between L_g and R_g.

The oceanic crustal model with 2-km-thick sediment and 4-km-thick basalt layers generates strong R_g but almost no L_g (Fig. 10). It is apparent from Figures 7 and 10 that this is in part due to the absence of Airy phases in the 3.1- to 3.7-km/sec L_g window, but it is also clear that what overtones are present do not have clustered Airy phases as do the thicker crustal models. This means that the absence of L_g is not just for the conventional window, but there is simply little possible oceanic L_g phase as a result of the wave-guide structure. The large amplitude of R_g implies an effect of trapping most of the fundamental mode energy in a narrow low-velocity layer, with the energy flux being much greater than that in the continental cases. In these theoretical calculations, which lack attenuation and scattering, R_g is predicted to be a dominant arrival for both oceanic and continental paths. In actuality, near-surface heterogeneities and attenuation tend to greatly reduce the short-period fundamental mode energy. Some of the R_g energy is probably scattered into the L_g phase (e.g., Gupta *et al.,* 1992), but even for the large amplitude R_g in the oceanic crust, this is not expected to significantly enhance L_g because the overtone modes simply do not exist to accommodate the scattered energy. For the oceanic structure, the S_n phase before the L_g window is very strong, especially for the radial component. We put in much effort to distinguish between L_g and R_g phases, because some researchers have neglected this problem in their simulations of L_g.

More Complex 1D Crustal Models

We have so far only considered the variation of crustal thickness and the effects of a single sediment layer. While we do not desire to be exhaustive in our analysis of complex wave-guide structures, it is instructive to consider somewhat more realistic models than used earlier. This is done using the normal-mode method for stratified media, with the waveforms filtered with a 0.3- to 1-Hz bandpass filter, so our synthetics are consistent with those of the finite-difference method.

First, we consider the "average" continental and oceanic models of Meissner (1986, p. 40), simplified to omit layering in the upper mantle. The corresponding continental *P*-wave velocity model is labeled model VI in Table 2. The waveforms calculated for this crustal model (Fig. 11a) have pulse-like L_g for vertical and tangential components with almost the same arrival time. Almost all of the guided wave energy, including fundamental-mode Rayleigh and Love waves, arrives within the L_g window. This is because there is no low-velocity surface layer in this model. The average oceanic model (Meissner, 1986) is shown as model III in Table 2, with the water layer being omitted. The energy distribution in the waveforms calculated for this model (Fig. 11b) is very different from that for the continental model. Because the sediment layer is thin (1 km) and has a very low velocity (v_s = 1 km/sec), significant energy is trapped in this layer. As a result, there is a very dispersed, complex fundamental mode signal for this structure. The wave train is very long. While our synthetics do not include attenuation, much of this short-period fundamental mode will be strongly attenuated in actual oceanic crust. There is no impulsive L_g phase in the conventional L_g window for the vertical component. For the *SH* component, there is considerable energy in this window, which involves the first two Love wave overtones.

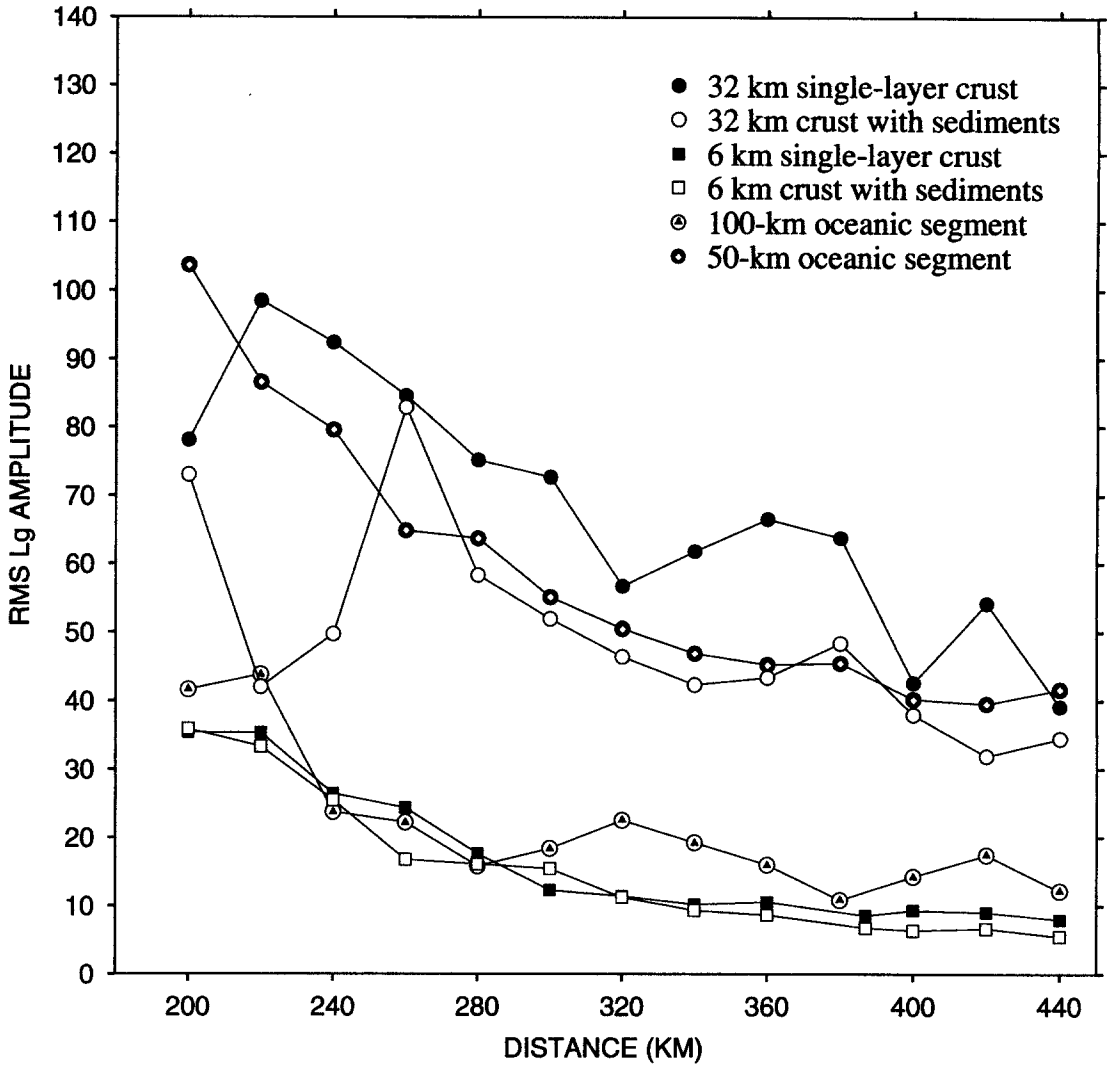

Figure 6. RMS amplitudes in the L_g window for vertical components for various models. The solid symbols are for the layer over half-space models. Circles and squares are for crustal thicknesses of 32 and 6 km. The open symbols are for the corresponding two-layer crustal models with low-velocity surface layers. The results of crustal thinning models are shown with other symbols. The open circles with solid triangles are for the 100-km-long oceanic segment model, measured in 3.7 to 3.2 km/sec window. The solid circles with white diamonds are for the 50-km-long oceanic segment model.

The group velocities are such that this energy does not separate clearly from the fundamental-mode Love wave.

We also considered oceanic crustal models with additional layers, to determine whether more complex structures could enhance oceanic L_g arrivals. Two models for the Pacific Ocean are shown as models IV and V in Table 2. The waveforms computed for these structures are shown in Figures 11c and 11d, identified as Pacific 1 (the four-layer crustal model of Shor *et al.*, 1970) and Pacific 2 (the five-layer crustal model of Hussong, 1972). The dispersion of low-velocity fundamental-mode energy is not as dramatic as for model III. The basic characteristics of the waveforms are similar: there is relatively little energy in the L_g window for the vertical component. However, the energy in this window for the *SH* component is substantial. The greater relative strength of the Love wave overtone energy in the oceanic crust may be part of the reason why transverse component calculations tend to underpredict L_g blockage, which is usually based on vertical component recordings.

These calculations with more complex crustal models indicate that the number of modes is not simply controlled by the layering of the structure. What is most important is the strength of velocity contrasts in the wave guide, and additional modes can be introduced by including larger internal velocity contrasts. If the deepest boundary has the strongest velocity contrast, the maximum number of normal modes is determined by the phase difference between a ray that has not suffered reflection and a ray that has suffered

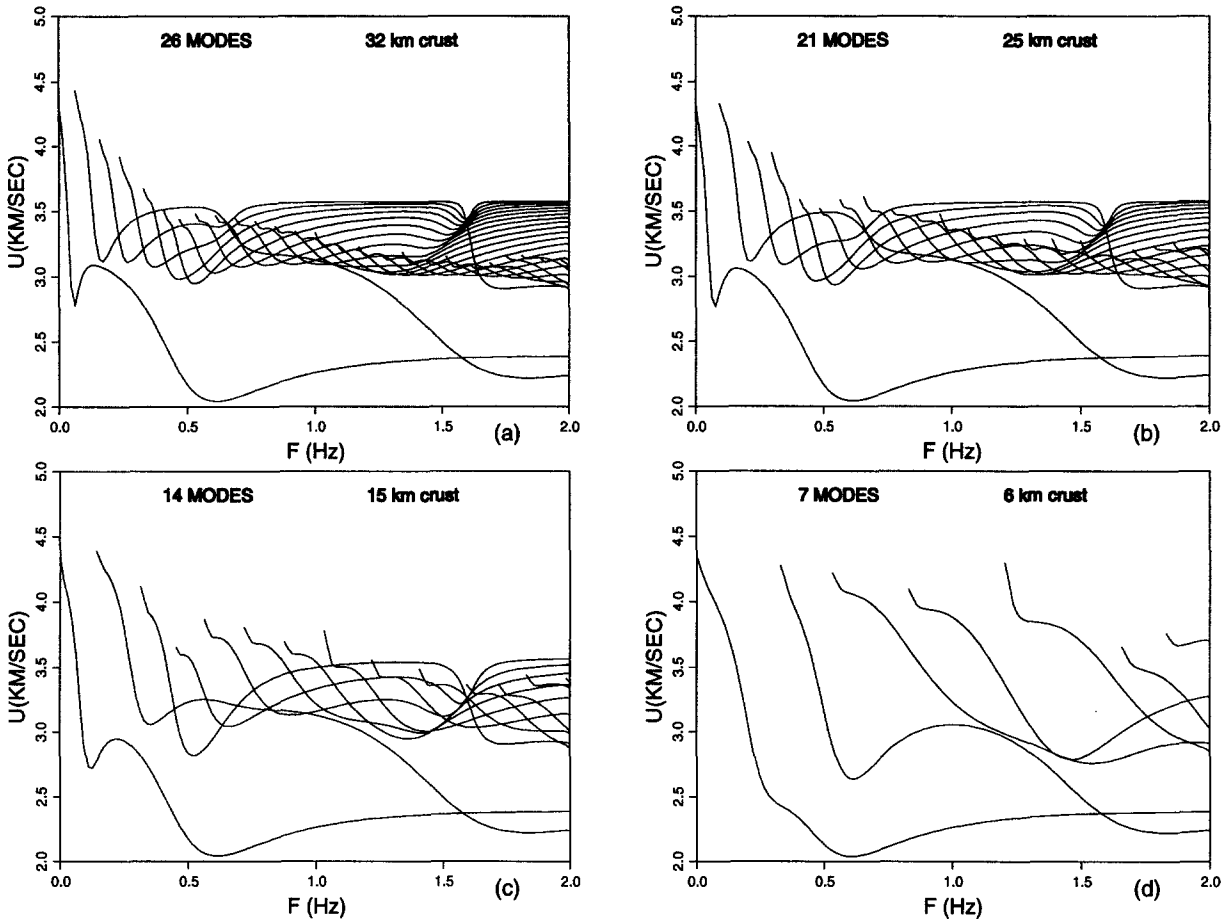

Figure 7. Dispersion curves for Rayleigh waves in two-layer crustal models with total crustal thicknesses of 32, 25, 15, and 6 km, with each model having a 2-km-thick low-velocity surface layer. Notice the additional Airy phase for the fundamental mode relative to Figure 2.

two total internal reflections. The relation is (Marcuse, 1991, p. 6)

$$(s_2 - s_1)k + \phi_2 + \phi_3 = 2N\pi, \qquad (3)$$

where s_1 is the distance traveled by the direct ray and s_2 is the distance traveled by the reflected ray, k is the wavenumber, $\phi_2 + \phi_3$ is the phase change resulting from the two total reflections, and N is the ordinal number of a normal mode. If the maximum phase difference increases to more than 2π, the number of modes will increase. The addition of extra layers could increase or decrease the maximum phase difference, so it may increase or decrease the number of normal modes. We calculated Love wave phase velocity dispersion curves in the frequency range 0 to 5 Hz for the four oceanic crustal models that we used to generate the synthetic seismograms in Figures 10 and 11. The numbers of crustal layers for each used model are 2, 2, 3, and 5. The corresponding numbers of normal modes are 19, 16, 13, and 15. Thus, there is not a simple increase in number of modes associated with more detailed layering.

The Effect of Crustal Thinning along a Path

In the previous section, we demonstrated that there is a fundamental difference in the modal structure for crust of different thickness, and this prevents stable propagation of L_g over long paths in oceanic structure. However, this leaves unclear the effect of a limited segment of thin oceanic crust along a continental path. We will explore this using the same two-dimensional finite-difference program used for the one-dimensional models considered previously.

We consider a crustal thinning model like that shown in Figure 1c. This model is almost the same as in Figure 1b of Cao and Muirhead (1993), except that our total model is shorter (450 km versus 600 km). The crustal thinning starts 50 km from the left of the model and reaches a minimum thickness of 6 km at 150 km from the left. The thin crust persists for the next 100 km. From 250 to 350 km, the thickness of the crust gradually increases to its original value of 32 km.

The finite-difference synthetics for a 5-km-deep source on the left side of this model are shown in Figure 12. If we compare this figure with Figure 3, the calculations for a uni-

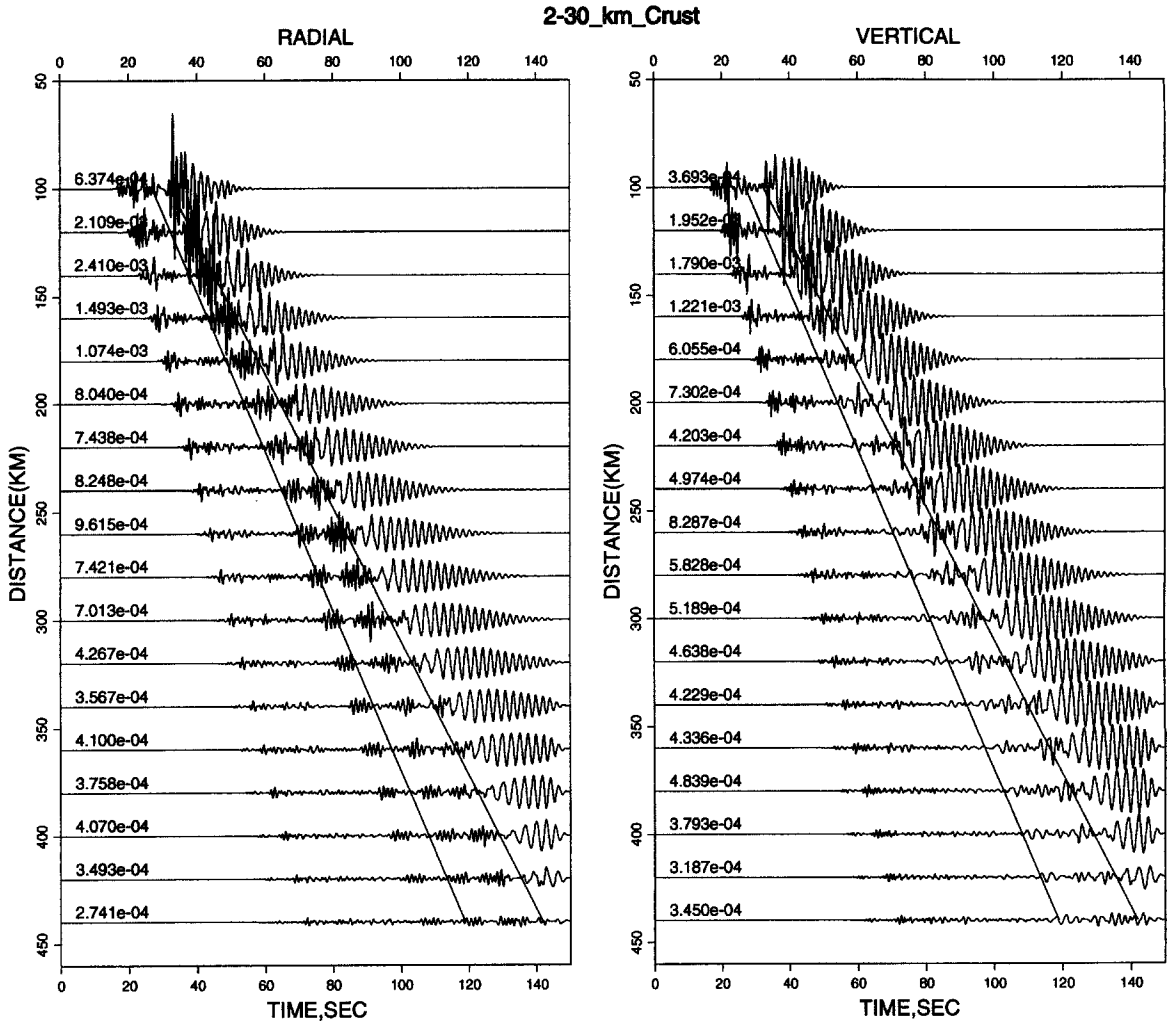

Figure 8. Synthetic seismograms for a two-layer crustal model with a thickness of 32 km, including a 2-km-thick sediment layer at the surface.

form 32-km-thick crust, and with Figure 5, the calculations for a uniform 6-km-thick crust, we find that the synthetics for the laterally varying structure are somewhat intermediate. There is slightly more energy within the L_g window in the laterally varying crustal model than for the purely oceanic structure, but not as much as for the uniform 32-km-thick model. For this single-velocity crustal model, R_g overlaps the latter part of the L_g window, especially within the stretches of thick crust. One has to carefully recognize the effects of R_g when assessing L_g blockage. If the window is slightly adjusted to avoid the R_g arrival (from 3.7 to 3.1 km/sec to 3.7 to 3.2 km/sec) the L_g amplitude reduction is seen to be stronger. There is about a factor of 4 reduction in the L_g amplitudes relative to the uniform 32-km-thick crust (Fig. 6). Cao and Muirhead (1993) correctly indicate that in a similar model, "higher modes of L_g are muted by the mantle uplift while the fundamental mode is left almost unchanged." However, they proceed to introduce a water column that effectively damps out R_g and indicate that this enhances the blockage of L_g. There is no need to introduce the water layer to affect L_g, because L_g has been largely disrupted by the crustal thinning alone. The dramatic effect on the overall waveform of scattering or attenuating R_g is easily misinterpreted as an affect on L_g. Using polarization analysis and frequency filtering allows the effects on L_g to be isolated.

As found in the last section, we can separate the L_g and R_g signals by introducing a low-velocity layer at the top of the crust. We consider models like Figure 1d, with a 2-km-thick sediment layer along the entire structure. In the zone of thinned crust, the basalt is 4-km thick. As expected, the R_g waves separate from the L_g window, L_g is blocked, and the resulting seismogram profile is quite similar to Figure 10 (the two-layered oceanic crustal model), so it is not shown here. If the segment of oceanic crust is only 50 km in length, there is much less attenuation of L_g, as shown by the RMS amplitudes in Figure 6 for a corresponding model. Since our results are quite consistent with those of Cao and Muirhead (1993), we do not explore the additional models that they considered, such as including a water layer.

It is clear that a 100-km-long segment of oceanic path

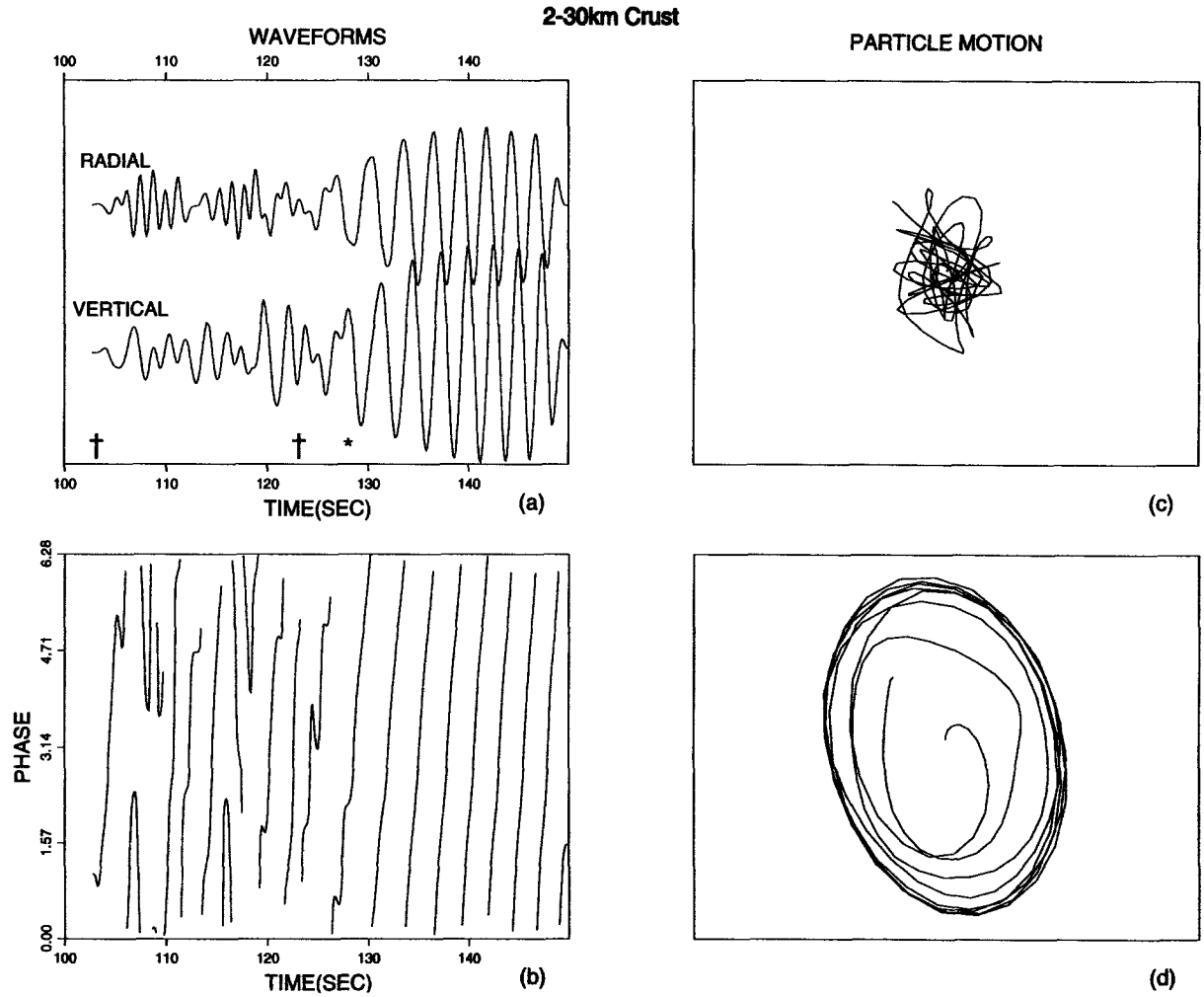

Figure 9. Particle motions of surface-wave arrivals for the waveforms at 380-km distance in Figure 8: (a) shows the waveforms of radial and vertical components. The asterisk marks a transition in characteristic particle motion. The L_g window is marked by two † symbols, and (b) is the polarization angle as a function of time. Both (c) and (d) are the particle motions before and after the asterisk. The latter shows almost perfect retrograde ellipse motion (R_g). The early window contains higher modes (L_g), characterized by the complex motion.

along an otherwise continental path can block *P–SV* type L_g rather efficiently.

Conclusions

Finite-difference and normal-mode calculations for simple crustal models clearly demonstrate that wave-guide structure, especially the overall thickness of the crust and the presence of any low-velocity surface layer, strongly affect the propagation of regional waves like L_g and R_g. For oceanic crust, due to the thin wave guide, the number of overtones is limited to only a few in a given frequency range. As a result, L_g is weak in oceanic structure because the higher-mode Airy phases do not cluster in group velocity to the extent that they do in thicker crust. The contribution of low-order overtones is somewhat higher for *SH* L_g than for *P–SV* L_g, in the 0- to 2-Hz passband. Our calculation shows that for crustal thicknesses in the range 15 to 32 km, L_g amplitudes are rather stable despite the variation of number of modes.

The presence of a low-velocity surface layer has several important effects. Because much of the short-period fundamental mode energy can be concentrated in a low-velocity surface layer, the R_g phase tends to separate from L_g for both oceanic and continental crusts with a sediment layer. Attenuation-free synthetics tend to be dominated by the strong dispersion and large amplitudes of R_g, but actual seismograms tend to show much weaker R_g. This is attributed to combined effects of strong attenuation and scattering in the shallow layer. While the scattered continental R_g phase may contribute to the L_g phase, this will not work very efficiently in an oceanic structure since the overtones are sparse.

Our calculations indicate that the lack of L_g signals for

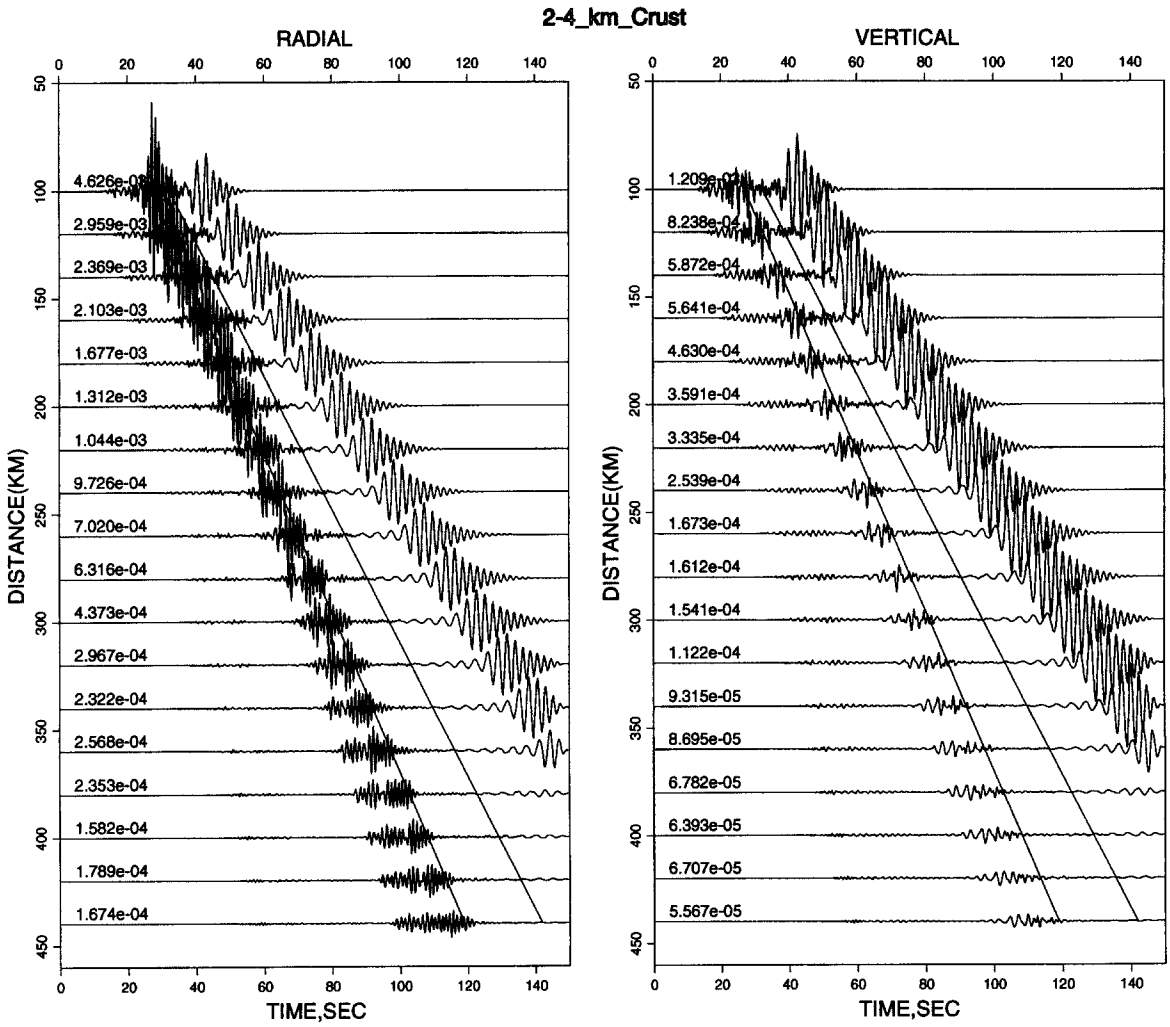

Figure 10. Synthetic seismograms for a two-layer crustal model, an overall 6-km crustal thickness including a 2-km sediment layer at the surface. The arrivals within the L_g window are weak. The R_g waves are delayed more for the two-layer model in Figure 5.

oceanic paths is primarily a gross structural effect, intrinsic to the thin wave guide. If frequencies higher than 2 Hz are considered, the presence of more overtones in the oceanic crust does allow L_g to develop, but there have not been very many observations of high-frequency oceanic L_g with which to assess the actual propagation efficiency. Two-dimensional models show that a 100-km-long segment of oceanic crust can reduce L_g amplitudes significantly, whereas a 50-km-long segment does not. This is consistent with previous modeling of *SH* L_g and indicates that there is a minimum path length required for the stabilization of the crustal modal structure, with the 100-km-long path being sufficient to act as a high pass filter on the regional signals.

Acknowledgments

We thank X.-B. Xie for providing us with the finite-difference codes. R. B. Herrmann kindly provided the codes used for calculation of dispersion curves. We make extensive use of the graphics software GMT provided by P. Wessel and W. H. F. Smith. This research was supported by the Air Force Office of Scientific Research under Grant F49620-94-1-0247. This is contribution number 263 of the Institute of Tectonics and the W. M. Keck Seismological Laboratory.

References

Aki, K. and P. G. Richards (1980). *Quantitative Seismology: Theory and Methods,* Vol. I, W. H. Freeman and Co., San Francisco, p. 264.

Birkeland, P. W. and E. E. Larson (1989). *Putnam's Geology.* Oxford University Press, Oxford.

Bostock, M. G. and B. L. N. Kennett (1990). The effect of 3-D structure on L_g propagation patterns, *Geophys. J. Int.* **101,** 355–365.

Brekhovskikh, L. M. (1980). *Waves in Layered Media,* Academic Press, New York.

Campillo, M. (1990). Propagation and attenuation characteristics of the crustal phase L_g, *Pure Appl. Geophys.* **132,** 1–19.

Campillo, M., B. Feignier, M. Bouchon, and N. Bethoux (1993). Attenuation of crustal waves across the Alpine range, *J. Geophys. Res.* **98,** 1987–1996.

Cao, S. and K. J. Muirhead (1993). Finite difference modeling of L_g blockage, *Geophys. J. Int.* **116,** 85–96.

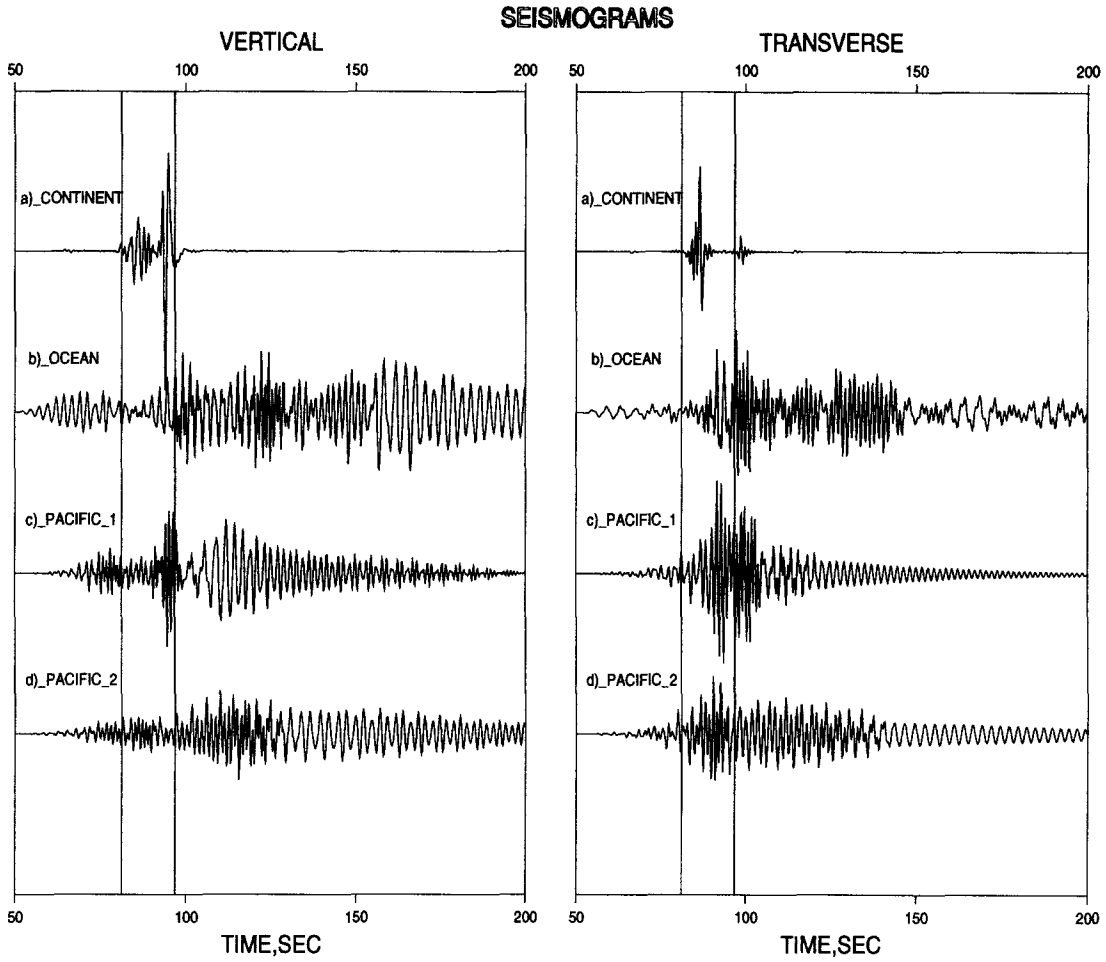

Figure 11. Synthetic seismograms for four crustal models at a distance of 300 km. They are (a) average continental crust from Meissner (1986), corresponding to model VI in Table 2; (b) average oceanic crust from Meissner (1986), corresponding to model III in Table 2; (c) a model for Pacific Ocean from Shor *et al.* (1970), IV in Table 2; and (d) another model for Pacific from Hussong (1972), V in Table 2.

Chazalon, A., M. Campillo, R. Gibson, and E. Garnero (1993). Crustal wave propagation anomaly across the Pyrenean Range—comparison between observations and numerical simulations, *Geophys. J. Int.* **115,** 829–838.

Ewing, M., W. S. Jardetsky, and F. Press (1957). *Elastic Waves in Layered Media,* McGraw-Hill, New York.

Gibson, R. L. Jr. and M. Campillo (1994). Numerical simulation of high- and low-frequency L_g-wave propagation, *Geophys. J. Int.* **118,** 47–56.

Gupta, I. N., W. W. Chan, and R. A. Wagner (1992). A comparison of regional phases from underground nuclear explosions at East Kazakh and Nevada test sites, *Bull. Seism. Soc. Am.* **82,** 352–382.

Herrmann, R. B. and C. Y. Wang (1985). A comparison of synthetic seismograms, *Bull. Seism. Soc. Am.* **75,** 41–56.

Hussong, D. M. (1972). Detailed structural interpretations of the Pacific oceanic crust using ASPER and ocean-bottom seismometer methods, *Ph.D. Dissertation,* 165 pp., University of Hawaii.

Israelson H. (1992). RMS L_g as a yield estimation in Eurasia, Final Report for AF Phillips Laboratory, Hanscom AFB, MA 01731–5000.

Kennett, B. L. N. (1986). L_g waves and structural boundaries, *Bull. Seism. Soc. Am.* **76,** 1133–1141.

Knopoff, L, R. G. Mitchel, E. G. Kausel, and F. Schwab (1979). A search for the oceanic L_g phase, *Geophys. J. Roy. Astr. Soc.* **56,** 211–218.

Knopoff, L., F. Schwab, and E. Kausel (1973). Interpretation of L_g, *Geophys. J. R. Astron. Soc.* **33,** 389–404.

Kock, W. E. (1965). *Sound Waves and Light Waves,* Anchor Books, New York.

Kovach, R. L. and D. L. Anderson (1964). Higher mode surface waves and their bearing on the structure of the Earth's mantle, *Bull. Seism. Soc. Am.* **54,** 161–182.

Marcuse, D. (1991). *Theory of Dielectric Optical Waveguides,* Academic Press, New York.

Maupin, V. (1989). Numerical Modeling of L_g wave propagation across the North Sea Central Graben, *Geophys. J. Int.* **99,** 273–283.

Meissner, R. (1986). *The Continental Crust,* Academic Press, New York.

Nuttli, O. W. (1986). Yield estimates of Nevada test site explosions obtained from seismic L_g waves, *J. Geophys. Res.* **91,** 2137–2151.

Panza, G. F. and G. Calcagnile (1975). L_g, L_i and R_g from Rayleigh modes, *Geophys. J. Roy. Astr. Soc.* **40,** 475–487.

Press, F. and M. Ewing (1952). Two Slow Surface Waves across North America, *Bull. Seism. Soc. Am.* **42,** 219–228.

Regan, J. and D. G. Harkrider (1989a). Numerical modelling of *SH* L_g waves in and near continental margins, *Geophys. J. Int.* **98,** 107–130.

Regan, J. and D. G. Harkrider (1989b). Seismic representation theorem

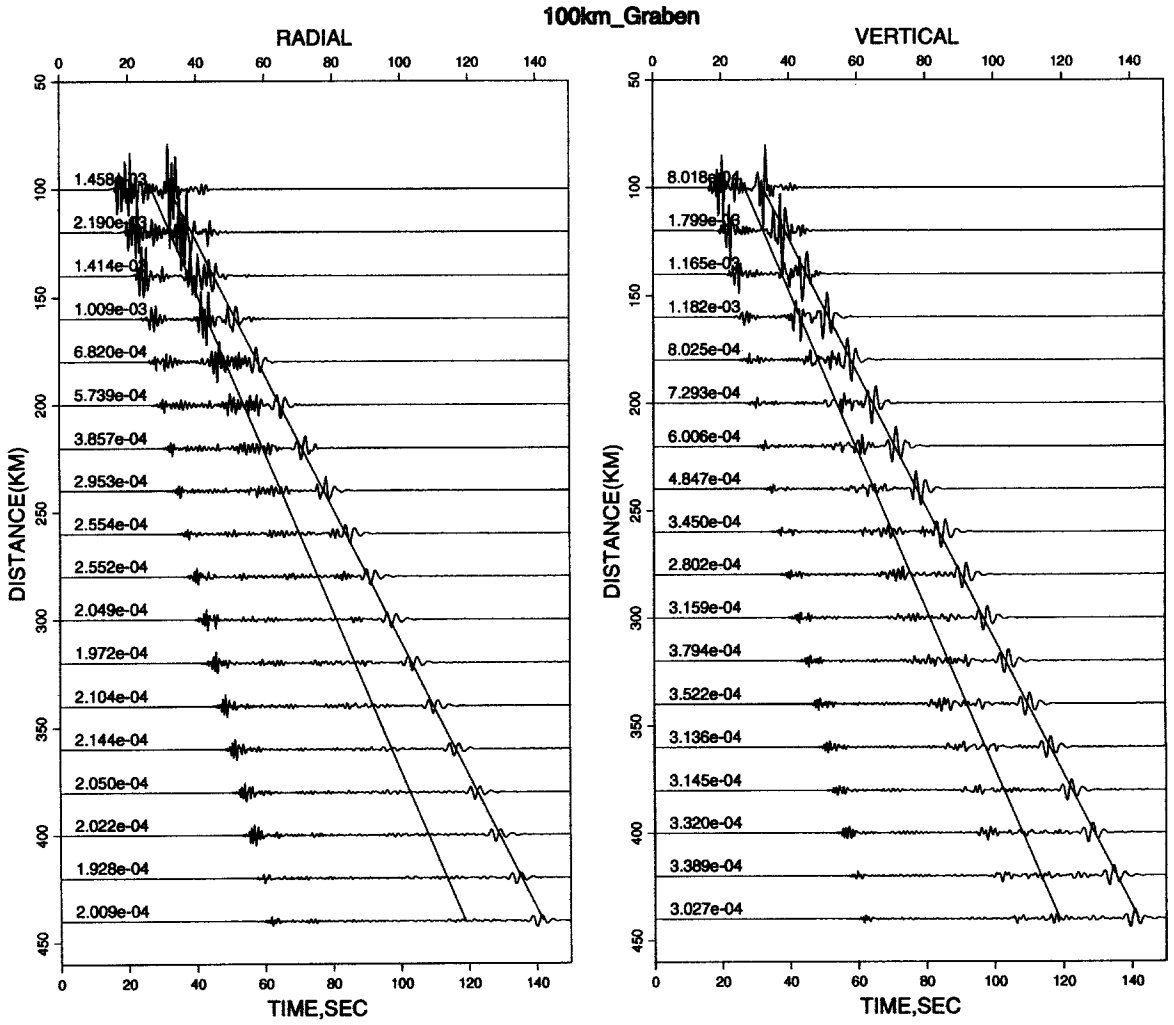

Figure 12. Synthetic seismograms for a one-layer crust model with variable crustal thickness as shown in Figure 1c. The crust is initially 32-km thick, then it begins to thin starting at 50 km from the left, becoming 6-km thick by 150 km from the left. This thickness persists from 150 to 250 km, then the crust begins to thicken from 250 to 350 km, recovering a 32-km thickness by 350 km.

coupling: synthetic SH mode sum seismograms for non-homogeneous paths, *Geophys. J. Int.* **98,** 429–446.

Shor, G. G. Jr., H. W. Menard, and R. W. Raitt (1970). Structure of the Pacific basin, in *The Sea,* A. E. Maxwell (Editor), vol. 4, part 2, Wiley-Interscience, New York.

Xie, X. B. and T. Lay (1994). The excitation of L_g waves by explosions: a finite-difference investigation, *Bull. Seism. Soc. Am.* **84,** 324–342.

Xie, X. B. and Z. X. Yao (1988). P-SV wave responses for a point source in two-dimensional heterogeneous media: finite-difference method, *Chinese J. Geophys.* **31,** 473–493.

Zhang, T. and T. Lay (1994a). Analysis of short-period regional phase path effects associated with topography in Eurasia, *Bull. Seism. Soc. Am.* **84,** 119–132.

Zhang, T. and T. Lay (1994b). Effects of crustal structure under the Barents and Kara seas on short-period regional wave propagation for Novaya Zemlya explosions: empirical relations, *Bull. Seism. Soc. Am.* **84,** 1132–1147.

Zhang, T., S. Y. Schwartz, and T. Lay (1994). Multivariate analysis of waveguide effects on short-period regional wave propagation in Eurasia and its application in seismic discrimination, *J. Geophys. Res.* **99,** 21929–21945.

Institute of Tectonics
University of California
Santa Cruz, California 95064
(T.-R.Z., T.L.)

Manuscript received 16 February 1995.